JOURNAL OF CATALYSIS 2, 274–298 (1963)

Investigation of the Mechanism of Chemisorption on Tungsten by Electrical Resistance Measurements

J. W. GEUS, H. L. T. KOKS, AND P. ZWIETERING

From the Central Laboratory, Staatsmijnen in Limburg, Geleen, The Netherlands

Received May 21, 1963

An extensive investigation was carried out into the influence of the adsorption of oxygen, carbon monoxide, nitrogen, and hydrogen on the electrical conductance of tungsten films obtained by evaporation. It appeared that tungsten films made in an ultrahigh vacuum on a glass surface with a temperature of about 288°K have a residual resistivity which exceeds the bulk resistivity at room temperature by a factor 20. Heating at 373°K for 16 hr hardly influenced the large surface area of the films, which amounted to 330–495 cm^2/mg tungsten, but reduced the residual resistivity to about 10 times the bulk value. From the kinetics of the decrease in resistance an activation energy of about 10 kcal/mole was obtained, which points to a defect-annealing mechanism.

In all cases chemisorption appeared to decrease the electrical conductance of the films. The fractional decrease in conductance was of the order of the ratio between the gas molecules adsorbed and the metal atoms present in the film.

The BET surface area of the films was measured by xenon adsorption. Chemisorption of oxygen and carbon monoxide decreased the BET surface area by about 20%, whereas hydrogen and nitrogen adsorption decreased it only by about 5%. This demonstrates the presence of very narrow pores in the films, the entrance to which is blocked to xenon atoms by chemisorbed oxygen or carbon monoxide.

To explain the experimental results, a detailed model of the films was developed. In this model the films are composed of rather large porous clusters of metal particles intimately grown together. The clusters are connected by isolated particles of the same size as the mean particle size in the film. Adsorption on these particles influences the conductance of the films, which implies that the effect of chemisorption on the metallic properties is localized.

The decrease in conductance was determined to an important extent by the distribution of the admitted gas molecules over the internal surface of the film. The sticking probability, its decrease with increasing coverage, and the mobility of adsorbed species over the surface were reflected in the rate and the total amount of the decrease in conductance.

The experiments with oxygen showed that at 273°K oxidation proceeds beyond a monolayer, whereas below 200°K, after a monolayer coverage, oxygen is only physically adsorbed. At 77°K simultaneous adsorption of nitrogen in two very different states was clearly demonstrated as well as the dependence of the ratio of these states on previous saturation at higher temperatures.

The most natural way to explain the experimental results is to assume that chemisorption affects the collective metallic properties mainly by changing the intermetallic forces between the surface atoms and the other part of the lattice. In hydrogen adsorption, the intermetallic bonds are only slightly weakened, whereas chemisorption of the other gases brings about such displacements of surface atoms that their contribution to the conductance is discontinued. The large effect per adsorbed nitrogen molecule at 273°K is attributed to the very specific sites on the metal surface to which adsorption of this gas is restricted at this temperature.

INTRODUCTION

To elucidate the role played by the metal in the chemisorption process many measurements have been made of the change in electrical conductivity of evaporated metal films (*1–15*).* The results of these measurements have mostly been explained by a change in the specific conductivity, which was ascribed to a variation in the number of conduction electrons (*2*, *3*, *6*). Besides, Sachtler and Dorgelo (*8*) attributed the change in resistance to the fact that, in the chemisorption process, the surface metal atoms lose their metallic properties and become nonconductive. The arguments in favor of either mechanism are inadequately supported by experimental evidence, and before conclusions about the chemisorption mechanism can be drawn from these measurements, more research remains to be done on the electrical properties of porous evaporated metal films upon adsorption. In a review of some mechanisms explaining the effect of chemisorption on the resistance of these metal films, Ehrlich also stressed the need for more experimental material (*16*).

A metal very well suited for this work is tungsten. The adsorption of many gases on tungsten was examined in detail by different methods, and clean films with a large and relatively stable surface area could be easily obtained. When we started our measurements on the resistance of tungsten films, no other work on this subject had been published. Shortly before our work was finished a paper of Suhrmann and co-workers appeared which contained measurements in accordance with our results (*15*).

I. METHODS

An accurate investigation into the effects of adsorption on the electrical resistance requires a metal sample with a large surface area in a perfectly clean condition. A metal film evaporated on a cooled substrate in an ultrahigh vacuum from a previously carefully degassed filament fulfils these requirements.

a. Materials

The films used in this work are evaporated from 0.2-mm tungsten wire (Drijfhout, Amsterdam; spectroscopically pure). Previously heating the wire in a separate apparatus at 10^{-6} mm Hg removes impurities from its surface. After this treatment the black appearance changes into a bright metallic one.

Oxygen is obtained by heating thoroughly degassed potassium permanganate, and carbon monoxide by decomposing formic acid with phosphoric acid at 150–180°C, followed by drying and purification over potassium hydroxide (mass-spectrometric analysis showed an oxygen content of 0.05%). Hydrogen is purified by diffusion through palladium or nickel; and nitrogen is prepared by decomposition of degassed sodium azide. The resulting nitrogen is adsorbed on silica at 77°K and hydrogen impurities, if any, are pumped off. Mass-spectrometrically, only 0.016% oxygen could be found. The xenon used for the determination of the BET surface area was obtained from Air Liquide. Analysis showed the presence of 0.93% Kr, 0.17% H_2, 0.09% N_2, and 0.02% O_2. This gas is further purified by pumping at 90°K till a vapor pressure of 6.1×10^{-2} mm Hg is observed [after correction for thermal flow (*17*, *18*)].

b. Ultrahigh Vacuum Techniques

Figure 1 represents the apparatus used in this work. Before the deposition of the film the measuring cell (A) is evacuated through the magnetically operated valve (B) filled with indium on the left side. The measuring cell may be isolated from the pumps by this valve, which has a large conductance when open, and can withstand atmospheric pressure after solidification of the indium without measurable leakage, provided the indium is handled carefully. To ensure that the glass is wetted by the indium the formation of an indium oxide layer on the glass should be prevented. To this end also the closing device is filled with indium so that the essential parts of the glass are permanently covered with the

---

* Only the literature of the last seven years has been cited.

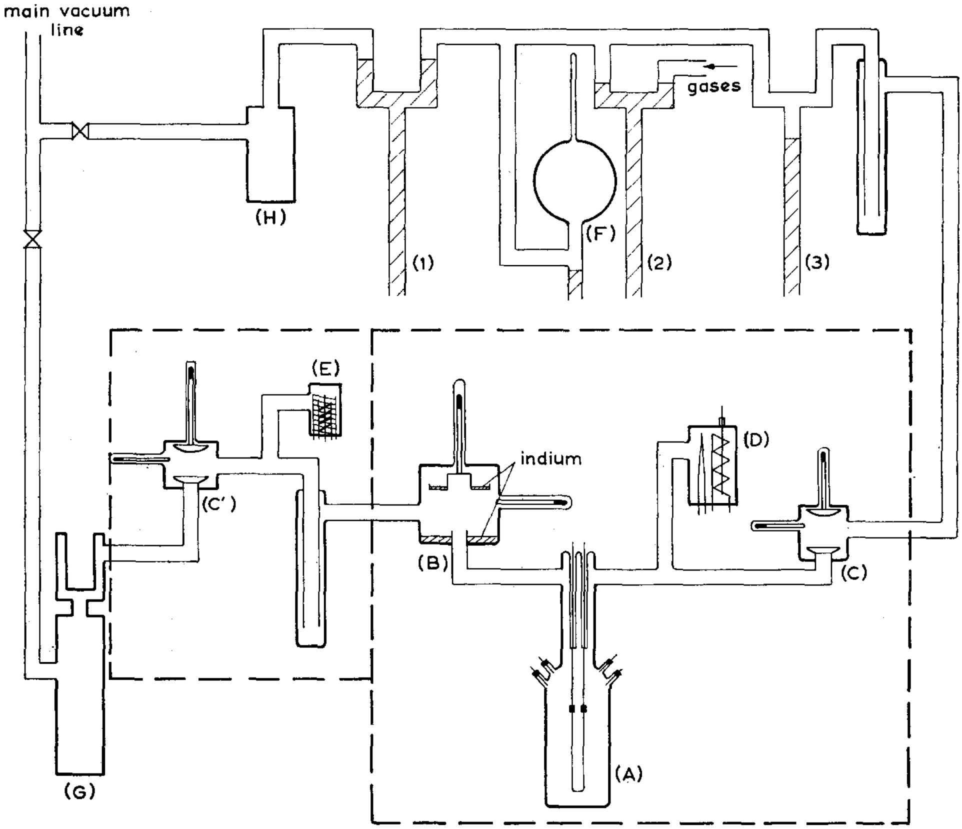

FIG. 1. Experimental apparatus. A. Measuring cell. B. Indium valve, magnetically operated. C, C'. Ground-glass balljoint shutters. D. Alpert-Bayard ionization gauge. E. Conventional ionization gauge. F. McLeod gauge. G. All-glass mercury diffusion pump, Venema and Bandringa (*19*). H. Small glass mercury diffusion pump. (1), (2), (3) Mercury cutoffs.

metal. After this valve has been closed, a gas pressure can be maintained over the film without any loss on the pump side. The other side of the measuring cell is connected to the gas-metering system by a greaseless glass balljoint shutter (C). When the pressure at either side of this shutter is kept at 10^{-6} mm Hg or lower, leakage is negligible.

The metering system is evacuated by a separate small glass mercury diffusion pump (H). The pressure of the admitted quantities of gas is measured by a McLeod gauge (F). To prevent contamination the gases are handled by mercury cutoffs. Before the gases enter the measuring cell the mercury vapor is removed by a trap cooled at 195°K.

To diminish the gas evolution of the walls the enclosed part of the apparatus is baked out at 300–400°C. Pumping was effected by an all-glass mercury diffusion pump (G), designed by Venema and Bandringa (*19*), backed by a metal mercury diffusion pump and a rotary oil pump of the main vacuum line. During the bake-out the pressure in the system is mainly determined by the adsorption of carbon dioxide, carbon monoxide, water, and nitrogen in the cold traps. When the adsorption in the cold trap approximates saturation, the pressure varies with the level of the liquid nitrogen in the trap. Then the pressure is determined not only by the transport of gases to the trap, but also by the adsorbing surface area. Since the pumping speed is proportional to the adsorbing surface area, the pressure determined by the equilibrium between desorption from the walls and filaments and the pumping speed also varies. In order to maintain the high adsorption power of the trap it is necessary to bake the entire apparatus after the mercury diffusion pumps, including the end part of the diffusion pump itself. The end part of the pump and the trap on the pump are for a short time baked out with thermal tape. To prevent large amounts of mercury penetrating into the apparatus, this is disconnected from the pump by a balljoint shutter (C^1) during the bake-out of the first trap (G). Then the first trap is cooled again, the balljoint shutter is opened, and pumping is continued.

After the first bake-out period the tungsten wire is reduced by electrically heating in hydrogen of 0.1–2 cm Hg. Subsequently, the system is again baked out and the metal parts are degassed. The Alpert-Bayard ionization manometer (D) is degassed by an electron bombardment with a maximum emission current of 25 ma at 650 volts. The tungsten filament is electrically heated by a current of about 4 amps. To degass also the end of the filament each platinum-iridium clamp holding the tungsten wire is connected with two tungsten leads clad with glass as far as possible (not shown in the figure). These leads also enable the clamps to be heated during degassing so that the ends of the filament are at a higher temperature during degassing than during evaporation, when the clamps are not heated. This procedure, published by Sachtler and Dorgelo (*4*), prevents desorption of gas from the end parts of the filament, when its temperature is increased. After the metal parts have been degassed, the apparatus is again baked out, the heating of the metal parts being only moderated but not stopped to avoid readsorption of gas. During this bake-out the pressure is measured by a conventional ionization gauge (E).

At the end of this cycle, when all parts, except the first trap, are hot, the pressure is about 5×10^{-7} mm Hg. After cooling of the second trap to liquid-nitrogen temperature the pressure is in the 10^{-8} mm Hg range. When the measuring cell is at room temperature and the Alpert-Bayard ionization gauge is switched on, the pressure is less than 10^{-9} mm Hg while the tungsten filament is still hot.

c. Evaporation of the Films

The films are deposited on the cylindrical wall of the measuring vessel. Two types of cells were used: one with a 3.2 cm diameter and one with a 5.8 cm diameter. In both cases the film was about 7.5 cm high. Generally 10–20 mg of tungsten are evaporated in 1 hr. During the evaporation the cell wall is cooled with streaming water at about 15°C. The filament is heated by a current of about 6 amps. When the current is raised to this value, the pressure rises momentarily to $1\text{–}2 \times 10^{-9}$ mm Hg to drop after some seconds to below 1×10^{-9} mm Hg. Then the measuring cell is disconnected from the pumps by the indium valve. Since the indium already melts at 150°C the valve closure needs no excessive heating of the glass walls which could cause a rise in pressure.

During the depositing of the film its resistance gradually decreases; no abrupt decrease, as is reported for other metals, is observed (*20*). Only one film is obtained from each tungsten filament; after each measurement a new filament is mounted.

d. Measurement of the Film Resistance

In this investigation the electrical resistance of the films was measured in two different ways: viz., by a Wheatstone-bridge method and by a compensation method. In both cases the influence of thermal emf is eliminated by commutation. In the first method contact with the film is established through two platinum wires that are so melted to the glass walls that they are diametrically opposed and parallel to the cylinder axis. Use was made of cylindrical platinum wires of 0.2 mm diameter and semicylindrical platinum wires of 1 mm diameter.

The thinner wires generally give a better contact with the film. The current through the film is about 5 ma; a 200-fold variation in potential difference across the bridge does not lead to a different value for the resistance.

In measurements by the compensation method a glass rod mounted close to the wall prevents deposition of the film on one side of the wall over a narrow range parallel to the cylinder axis. On either side of this uncovered zone a 0.2-mm platinum wire is melted to the glass to carry the current to the film. Here the current is about 10 ma, and flows only in one direction. To measure the potential difference across the film, the film is connected to a Dieselhorst compensator by two previously evaporated platinum films. These narrow films are deposited diametrically on the cell wall and are well sintered.

When, upon adsorption, the change in resistance measured by the compensation method and that measured by the Wheatstone-bridge method between the platinum films are compared, the relative variation of the latter was always smaller, by at most 20%. The temperature coefficient of the resistance measured by the Wheatstone-bridge method is slightly higher than that measured by the compensation method.

With the semicylindrical wires the temperature variation of the resistance is anomalous and much greater; e.g., a 100°C temperature increase lowers an 11 ohm resistance by about 2 ohms. In this case the resistance variations with temperature are not quite reproducible; obviously additional electric resistances due to poor contacts between film and wires influence the measurement. However, the relative change in resistance per adsorbed molecule does not differ very much from the values obtained by the compensation method, when during the adsorption and the measurement the temperature is kept constant.

e. Determination of the Surface Area

The surface area of the films is determined, according to Brunauer, Emmett, and Teller (*21*), by measurement of the extent of the physical adsorption of xenon (*2*, *6*) at 90°K at relative pressures ranging from 0.05–0.30. To ensure equilibrium the pressures are measured about 15 min after the admission of the gas. The pressure readings are corrected for thermal flow by Liang's empirical expression, as modified by Bennett and Tompkins (*17*). Dead space amounts to about 1800 cm^3.

The effective surface area per xenon atom is determined from comparative measurements of the physical adsorption of krypton and xenon on carbonyl iron. If Livingston's value for the effective surface area of krypton (*22*) is accepted (18.5 Å^2), the value for xenon appears to be 22.4 Å^2. This value is in good accordance with Anderson and Baker's (*23*) value of 23 Å^2 based on geometrical arguments.

II. Results

a. Properties of the Films

When the resistance is measured immediately after evaporation as a function of temperature, in the range 77–290°K, a straight relationship is obtained in accordance with Matthiessen's rule (*24*) (Fig. 2). This indicates that the total resistance may be divided into a temperature-dependent ideal resistance brought about by the lattice vibrations of the metal, and a temperature-independent residual resistance, which is due to scattering of conduction electrons by lattice defects, grain boundaries, etc. As in both the bulk metal and the evaporated films the effect of temperature on the ideal resistance is brought about by the thermal vibrations of the metal atoms, the bulk value can be accepted for the temperature variation of the specific resistance (resistivity) of the films. Therefore we assume:

$$d\rho_f/dT = d\rho_b/dT$$

in which ρ_f is the resistivity of the film and ρ_b the resistivity of the bulk tungsten. From

$$R_f = (l_{\text{eff}}/O_{\text{eff}})\rho_f = G\rho_f$$

where R_f is the film resistance, l_{eff} the effective length, and O_{eff} the effective surface area (width times thickness) for the electricity transport, it follows that

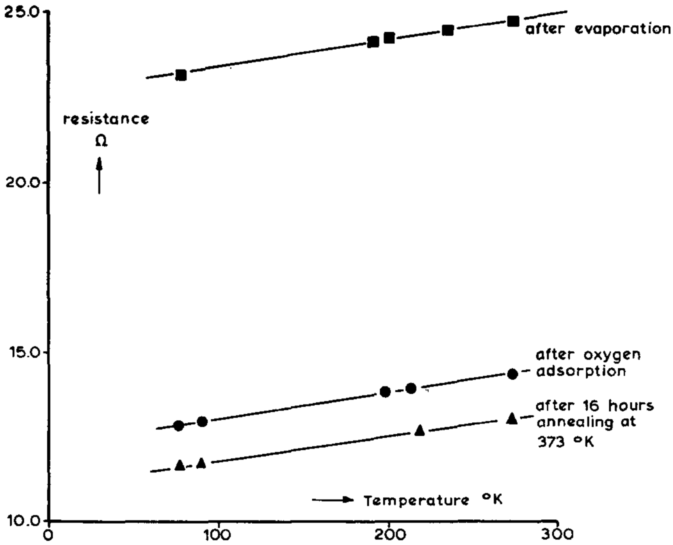

FIG. 2. Dependence on temperature of the resistance of film 1.08.

$$dR_f/dT = G\,(d\rho_b/dT)$$

hence

$$\frac{dR_f/dT}{d\rho_b/dT} = G = \frac{l_{eff}}{O_{eff}}$$

Consequently, an impression of the geometric factor G of the film can thus be obtained from the temperature variation of the resistance (*25, 26*). The temperature variation of the resistivity of bulk tungsten is (*27*):

$$d\rho_b/dT = 2.36 \times 10^{-8}\Omega\text{ cm °K}^{-1}$$

The geometric factor G enables the ideal resistance of the film to be calculated.

$$R_{id} = \rho_b G$$

in which ρ_b is the resistivity of bulk tungsten with a negligible amount of residual resistance, viz. (*27*),

$$\rho_b = 4.89 \times 10^{-6}\Omega\text{ cm at 273 °K}$$

In Table 1 all these data are collected for three films deposited in the 5.8 cm diameter cell; the residual resistivity is calculated from the difference in experimental and ideal resistance. From these data it can be concluded that at 273°K the residual resistivity is about 20 times the ideal resistivity; this indicates a highly distorted metal structure.

That the films do not have a compact platelet structure follows from the geometric factors in Table 2. The geometric factors for compact flat films with the same amount of tungsten on the same substrate as the experimental films, are also given in the table. For the films in the narrower cell the discrepancy is larger (about a factor 3) than for the films in the wider cell (about a factor 2). Hence, the devia-

TABLE 1

PROPERTIES OF TUNGSTEN FILMS AFTER DEPOSITION

Film no.	$R_{273°K}$ (Ω)	Temp. coeff. of resistance (% °K^{-1})	dR/dT (Ω°K^{-1})	Geometric factor (cm^{-1})	Ideal resistance (Ω)	Residual resistivity (Ω cm)
27	35.3	0.019	6.6×10^{-3}	2.8×10^{5}	1.4	1.2×10^{-4}
28	24.0	0.020	4.9×10^{-3}	2.1×10^{5}	1.0	1.1×10^{-4}
30	25.15	0.029	7.2×10^{-3}	3.1×10^{5}	1.5	8.1×10^{-5}
1.09	24.7	0.032	7.8×10^{-3}	3.3×10^{5}	1.6	7.0×10^{-5}

TABLE 2

Properties of Tungsten Film after 16 Hours' Annealing at 373°K[a]

Film no.	Film weight (mg)	$R_{273°K}$ before annealing (Ω)	$R_{273°K}$ after annealing (Ω)	Temp. coeff. of resist. (% °K⁻¹)	dR/dT (Ω°K⁻¹)	Geometric factor (cm⁻¹)	Geometric factor for platelet structure (cm⁻¹)	Ideal resistance (Ω)	Residual resistivity (Ω cm)
24	9.9	—	1.06	0.086	9.06×10^{-4}	3.84×10^{4}	—	0.18	2.27×10^{-5}
25	19.6	—	4.22	0.060	2.52×10^{-3}	1.07×10^{5}	3.47×10^{4}	0.52	3.45×10^{-5}
26	16.7	—	5.51	0.050	2.70×10^{-3}	1.14×10^{5}	4.07×10^{4}	0.56	4.35×10^{-5}
27	16.5	35.3	12.12	0.064	7.75×10^{-3}	3.28×10^{5}	1.53×10^{5}	1.61	3.22×10^{-5}
28	19.9	24.0	9.83	0.057_5	5.65×10^{-3}	2.40×10^{5}	1.27×10^{5}	1.18	3.60×10^{-5}
29	12.9	—	18.17	0.047	8.53×10^{-3}	3.62×10^{5}	1.96×10^{5}	1.77	4.53×10^{-5}
30	15.7	25.15	12.36	0.051_5	6.33×10^{-3}	2.68×10^{5}	1.61×10^{5}	1.31	4.08×10^{-5}
1.09	15.3	24.7	13.02	0.055_5	7.25×10^{-3}	3.07×10^{5}	1.65×10^{5}	1.50	3.76×10^{-5}

[a] Films 24, 25, and 26 were deposited in the narrow measuring cell; for film 24 a different contact electrode arrangement was used. The other films were *evaporated in the wide measuring cell.*

tion from a platelet structure is larger for the thicker films in the narrower cell.

After the evaporation the films are not stable and the resistance decreases spontaneously. If the process is assumed to be first order, a rough estimate of the activation energy of this process yields a value of 13 kcal/atom in the first stage of annihilation. This activation energy is high compared with values observed for gold, silver, and copper, viz., 2–4.5 kcal/atom (*28*), but this is quite acceptable in view of the high melting temperature of tungsten (*29*).

To avoid interference of this spontaneous decrease with the effects of adsorption on the resistance, the films are heated at 373°K for 16 hr before the influence of adsorption is measured. After this treatment the resistance again follows Matthiessen's rule in the temperature range 77–300°K. For the films deposited in the 3.2-cm measuring cell the decrease in resistance during the heat treatment is much less than for films evaporated in the 5.8-cm cell, viz., about 1 Ω for a resistance of about 5 Ω and 10–20 Ω for a resistance of 20–35 Ω, respectively. This indicates that the radiation of heat from the tungsten filament in the narrower cell already causes an annihilation of defects during the evaporation. The large decrease in resistance of the films deposited in the wider cells cannot be ascribed to the lower thickness of these films as rather thin films (weight: about 3 mg against 10–20 mg normally) in the narrower cell do not give a large decrease in resistance upon heating.

Table 2 gives the properties of films after heating at 373°K. From a comparison of the data in Tables 1 and 2 it appears that the residual resistivity is sharply diminished by heating whereas the geometric factor does not vary much. This is evidence that defects are only annealed during heating, which was already suggested by the still low value of the activation energy, which is in good agreement with Pierotti and Halsey's (*30*) and Anderson and Baker's (*23*) observations that the surface area of evaporated tungsten films did not decrease upon heating at 710° and 510°K, respectively.

TABLE 3

PROPERTIES OF TUNGSTEN FILMS AFTER CHEMISORPTION

Film no.	$R_{273°K}$ (Ω)	Temp. coeff. of resistance (% °K⁻¹)	dR/dT (Ω°K⁻¹)	Geometric factor (cm⁻¹)	Ideal resistance (Ω)	Residual resistivity (Ω cm)	Surface area (cm² mg⁻¹)	Gas adsorbed	α $\left(\frac{\text{Metal atoms}}{\text{Adsorbed molecules}}\right)$
24	1.18	0.086_5	1.02×10^{-3}	4.32×10^{4}	0.211	2.24×10^{-5}	200	O_2	2.6
25	4.83_5	0.059	2.86×10^{-3}	1.22×10^{5}	0.59_5	3.48×10^{-5}	270	O_2	2.1
26	—	—	—	—	—	—	320	O_2	2.6
27	13.06	0.062_5	8.15×10^{-3}	3.45×10^{5}	1.69	3.30×10^{-5}	235	CO	2.3
28	11.12	0.077_5	6.40×10^{-3}	$2.71 \times 10_5$	1.33	3.62×10^{-5}	210	O_2	2.6
29	19.78	0.046	9.05×10^{-3}	3.84×10^{5}	1.88	4.66×10^{-5}	265	CO	2.2
30	13.55	0.054	7.30×10^{-3}	$3.09_5 \times 10^{5}$	1.51	3.90×10^{-5}	255	CO	2.2
1.09	14.39	0.055	8.0×10^{-3}	3.40×10^{5}	1.66	3.75×10^{-5}	250	O_2	2.6

The surface area of our films is much larger than the geometrical area on which the film is deposited, viz. 5000 cm² against about 100 cm². Like the geometrical factor, this, too, points to the films not having a compact structure. The surface area is roughly proportional to the weight of tungsten evaporated; all values measured are between 300 and 500 cm²/mg of tungsten. Anderson and Baker (*23*) measured values in the same range for films evaporated on the wall of a 7.6 cm diameter vessel.

After adsorption the resistances again follow Mathiessen's rule within the experimental accuracy. In Table 3 the data are collected. The increase in resistance of about 10% by the adsorption of oxygen, carbon monoxide, and nitrogen causes the slope of the resistance–temperature curve also to increase by about 10%, which, for the time being, is expressed as a change in the geometric factor. No change in residual resistivity is detected beyond the experimental error.

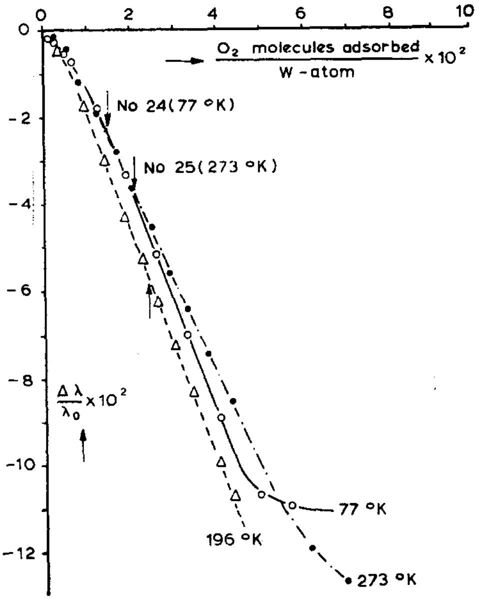

FIG. 3. Effect of oxygen adsorption on the conductance of evaporated tungsten films at 77°, 195°, and 273°K. ○, Film no. 24; 252 cm²/mg; α = 2.56 (77°K). △, Film no. 26; 403 cm²/mg; α = 2.67 (195°K). ●, Film no. 25; 340 cm²/mg; α = 2.15 (273°K). ↓, Adsorption of 2 × 10¹⁴ molecules/cm².

b. *Effect of Oxygen Adsorption*

In Fig. 3 the influence of oxygen adsorption on the conductance at three temperatures is represented by plotting the relative decrease in conductance $\Delta\lambda/\lambda_0$ versus the number of oxygen molecules adsorbed per tungsten atom.

In the first stage of the process, in which about 5×10^{14} oxygen molecules/cm^2 are adsorbed, the adsorption is immeasurably fast, while the conductance also decreases very fast. At 77° and 195°K more gas is still rapidly adsorbed, after the adsorption of about 5×10^{14} molecules/cm^2, but the conductance does not change any more. At 273°K the adsorption of more gas is slow and the conductance decreases linearly with the amount adsorbed.

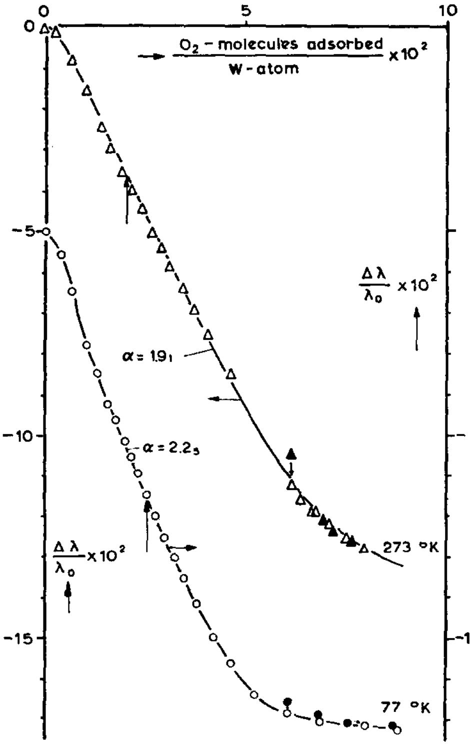

FIG. 4. Comparison of effects of oxygen on the conductance at 77° and 273°K. Further oxidation at 273°K. ● ○, Film no. 1.07; 420 cm^2/mg; (77°K). ▲ △, Film no. 1.06; 335 cm^2/mg; (273°K). ● ▲, Immediately after admission of oxygen. ○ △, After equilibration. ↑, Adsorption of 2×10^{14} molecules/cm^2.

At all temperatures investigated in the initial stage the decrease in conductance per oxygen molecule adsorbed is relatively small. Afterwards the conductance decreases linearly with the amount of oxygen adsorbed. The slope of the straight part of the curve is of the order of unity, which means that the change in relative conductance is of the order of the number of oxygen molecules adsorbed per tungsten atom. At 273°K the slope is less than at 77°K and 195°K, viz. 2.1 versus 2.6.

During the slow adsorption at 273°K the decrease in conductance is again linear with the amount of oxygen adsorbed, but now the slope of the curve is less. This is illustrated by the measurements of Fig. 4. These measurements, in contrast to those in Fig. 3, are made by the Wheatstone-bridge method. Owing to the contact resistance between film and platinum wires,

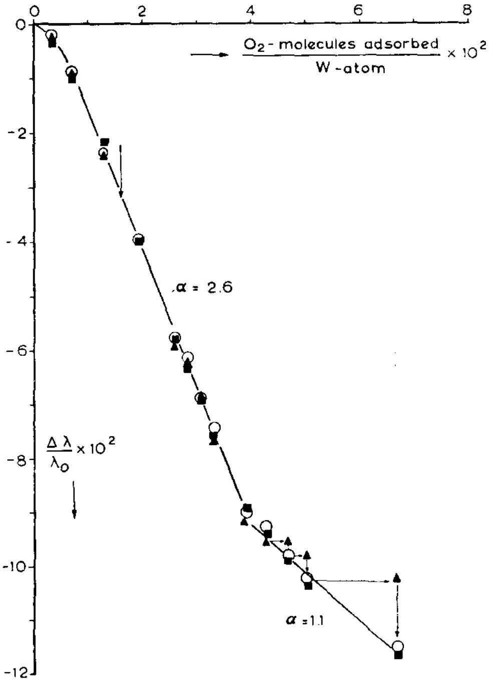

FIG. 5. Effect of oxygen admitted at 77°K on the conductance measured at 77°K and 273°K. Film no. 28; 265 cm^2/mg; ▲, measured at 77°K after admission at this temperature; ■, measured at 273°K after admission at 77°K; ○, measured at 77°K after recooling; ↑, adsorption of 2×10^{14} molecules/cm^2.

which does not change on adsorption, the slope is now slightly less, viz. 1.91 at 273°K and 2.25 at 77°K.

Figure 5 shows an experiment in which the oxygen is admitted at 77°K and the conductance is measured at 77°K and 273°K. Heating to 273°K and recooling to 77°K has no effect on the conductance, which indicates that equilibrium is attained at 77°K. At both temperatures the slope of the straight part of the curves is the same, 2.6, which corresponds with the above values measured at 77° and 195°K. After 5×10^{14} oxygen molecules/cm^2, which is roughly equivalent to one monolayer of oxygen atoms, have been adsorbed, still more oxygen is rapidly adsorbed at 77°K, but the conductance remains constant. When the temperature is raised to 273°K the pressure at first increases owing to the desorption of physically adsorbed gas and then decreases again slowly, while the conductance decreases accordingly. Here, too, a linear decrease in conductance is observed which has a smaller effect per oxygen atom, viz. 1.15, than that observed in the first straight part.

Cooling again to 77°K has no influence upon the decrease in conductance.

c. *Effect of Carbon Monoxide Adsorption*

Measurements of the influence of carbon monoxide adsorption are collected in Fig. 6. These measurements are carried out by the Wheatstone-bridge method. Although the adsorption of gas is immeasurably fast, the conductance decreases slowly, at a rate which becomes lower as more gas is adsorbed, which is in contrast to what has been found in oxygen adsorption. At all adsorption temperatures the conductance curves are again flat at first, but afterwards show a linear decrease with the number of carbon monoxide molecules adsorbed. Also in this case the slope of this linear part varies with the adsorption temperature, but now the slope is weaker at 77°K than at 273°K, viz. 1.1 and 1.9 respectively, which is in contrast to what has been observed in oxygen adsorption. At 195°K an intermediate value of 1.5 is observed. Also the maximum decrease in conductance is lower in the measurements at 77°K, viz. 8% against 10% at 273°K.

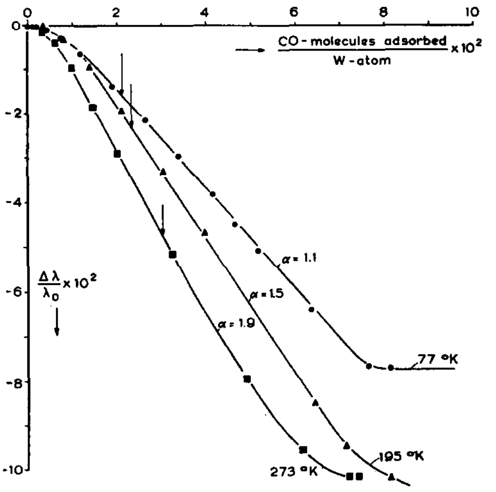

FIG. 6. Effect of carbon monoxide adsorption at 77°, 195°, and 273°K on the conductance of evaporated tungsten films. ●, Film no. 9; 345 cm^2/mg; (77°K). ▲, Film no. 10; 384 cm^2/mg; (195°K). ■, Film no. 11; 495 cm^2/mg; (273°K). ↑, Adsorption of 2×10^{14} molecules/cm^2.

After adsorption of 7×10^{14} molecules/cm^2 at 77°K and of 4×10^{14} molecules/cm^2 at 195° and 273°K the conductance re-

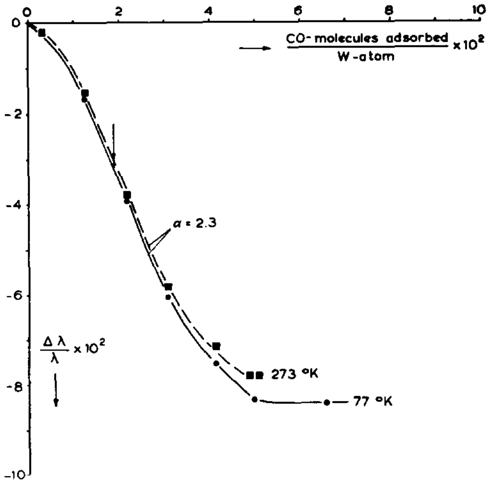

FIG. 7. Effect of carbon monoxide admitted at 273°K on the conductance measured at 77° and 273°K. Film 27; 295 cm^2/mg; ■, measured at 273°K after admission and after cooling to 77°K; ●, measured at 77°K after admission at 273°K; ↑, adsorption of 2×10^{14} molecules/cm^2.

mains constant, although still more carbon monoxide is rapidly adsorbed. Figure 7 represents a measurement in which carbon monoxide is admitted at 273°K, and the conductance is measured both at 273°K and 77°K. Unlike the measurements of Fig. 6, these measurements were done by the compensation method. At either temperature the slope of the linear part is the same; at 77°K more gas is adsorbed and the conductance further decreases along the same line. When the film is heated again to 273°K, the conductance returns to the value it had before cooling, and the total amount of additional gas desorbs.

These results were exactly reproduced on two other films (Table 4, Nos. 27, 29, 30). By elimination of the contact resistance higher slopes were obtained, viz. 2.2 against 1.9 in the Wheatstone-bridge measurements.

d. Effect of Nitrogen Adsorption

Measurements on the effects of nitrogen adsorption are given in Fig. 8. When nitrogen is admitted at 273°K and the conductance is measured at 77° and 273°K the

TABLE 4
SUMMARY OF THE EFFECT OF CHEMISORPTION ON THE CONDUCTANCE OF EVAPORATED TUNGSTEN FILMS

Film no.	Measuring temp. (°K)	Gas adsorbed at (x) °K	$\alpha \left(\frac{\text{Metal atoms}}{\text{Gas molecules ads.}}\right)$	Measuring method
9	77	CO	1.1	Wheatst.
13	77	CO	1.2	Id.
15	77	CO	1.3	Id.
10	195	CO	1.5	Id.
16	195	CO	1.5	Id.
11	273	CO	1.9	Id.
12	273	CO	1.8	Id.
14	273	CO	1.6	Id.
27	273	CO (273)	2.3	Comp.
	77		2.3	
29	273	CO (273)	2.2	Id.
	77		2.2	
30	273	CO (273)	2.2	Id.
	77		2.2	
24	77	O_2	2.6	Id.
1.07	77	O_2	2.3	Wheatst.
1.02	77	O_2	2.8	Id.
26	195	O_2	2.6	Comp.
1.08	195	O_2	2.6	Wheatst.
1.06	273	O_2	1.9	Id.
25	273	O_2	2.1	Comp.
28	77	O_2 (77)	2.6	Id.
	273		2.6	
1.09	77	O_2 (77)	2.6	Id.
	273		2.45	
17	77	H_2	0.5	Wheatst.
18	77	H_2	0.5	Id.
19	273	H_2	0.8	Id.
1.01	273	H_2	0.9	Id.
1.11	273	H_2	0.9	Comp.
20	273	H_2	1.0	Wheatst.
21	77	N_2	1.2[a]	Id.
34	77	N_2	1.0[a]	Comp.
33	77	N_2 (273)	3.8	Id.
	273		4.0	

---

[a] No linear part.

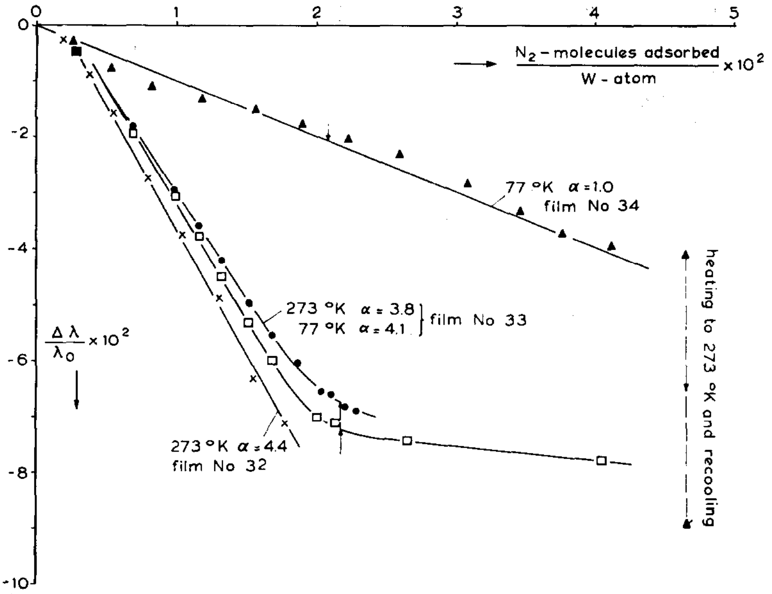

FIG. 8. Effect of nitrogen adsorption at 77° and 273°K on the conductance of evaporated tungsten films. Film no. 32 surface area not determined; gas admitted and conductance measured at 273°K, ×. Film no. 33, 355 cm^2/mg; gas admitted at 273°K; conductance measured at 273°K, ○; conductance measured at 77°K, □. Film no. 34 340 cm^2/mg; gas admitted and conductance measured at 77°K, △; conductance measured at 77°K after heating to 273°K, △̸. ↑, Adsorption of 2×10^{14} molecules/cm^2.

decrease in conductance is the same at both temperatures till about 2×10^{14} molecules/cm^2 have been adsorbed. At 273°K the last quantities of gas are adsorbed more and more slowly and the conductance decreases likewise.

If, after adsorption at 273°K has stopped, the temperature is lowered to 77°K another amount of gas approximately equal to that adsorbed at 273°K is rapidly adsorbed. This adsorption proceeds without a marked decrease in conductance.

The slope of the straight part of the curve is rather high, about 4, and the corresponding decrease in conductance is about 8%, when only 2×10^{14} nitrogen molecules/cm^2 have been adsorbed.

Nitrogen adsorbed at 77°K influences the conductance in a different way. Now the maximum decrease of the conductance is about 4% only. At the start and towards the end of the adsorption the conductance drops slightly more rapidly; the curve does not exhibit a linear part. When, after completion of the decrease in conductance, the film is heated to room temperature and cooled again to 77°K, the decrease in conductance, about 9%, is much larger whereas the amount of gas adsorbed remains the same.

e. *Effect of Hydrogen Adsorption*

The measurements of the effects of hydrogen adsorption are collected in Fig. 9. At 273° and 373°K the conductance decreases linearly with the amount adsorbed from the start. At 77°K a flat part may be distinguished, but this is not very pronounced. Just as for carbon monoxide adsorption the slope of the linear parts of the curves increases with measuring temperature, viz. from 0.55 at 77°K to 1.0 at 373°K. In agreement with the low slopes for this gas the maximum decrease in conductance is low. After about 5×10^{14} hydrogen molecules/cm^2 have been adsorbed, the total decrease in conductance is only about 3%, whereas the same number of oxygen or carbon monoxide molecules adsorbed per cm^2 give rise to a decrease of

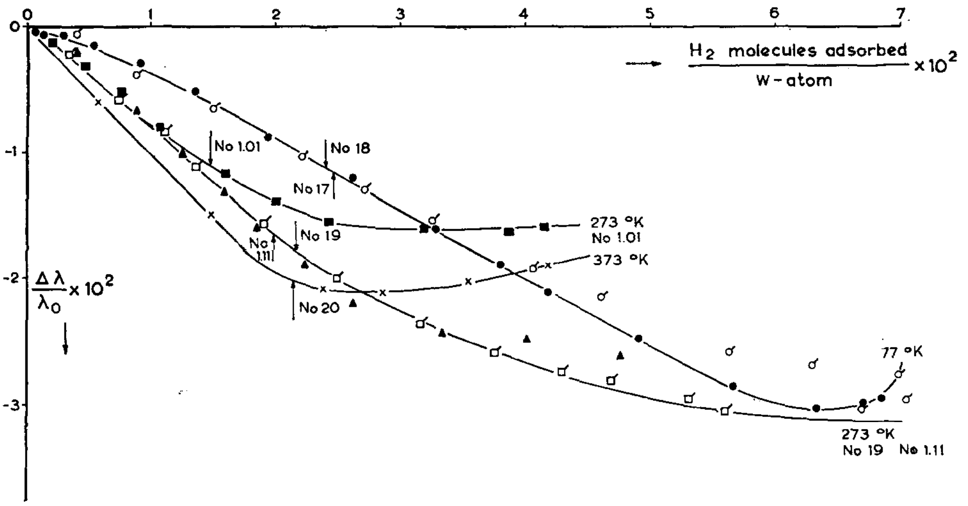

FIG. 9. Effect of hydrogen adsorption on the conductance of evaporated tungsten films at various temperatures. ×, Film no. 20; 350 cm²/mg; 373°K; $\alpha = 1.0$. □́, Film no. 19; 355 cm²/mg; 273°K; $\alpha = 0.85$. ▲, Film no. 1.11; 325 cm²/mg; 273°K; $\alpha = 0.85$. ■, Film no. 1.01; 210 cm²/mg; 273°K; $\alpha = 0.85$. ●, Film no. 17; 370 cm²/mg; 77°K; $\alpha = 0.55$. ○́, Film no. 18; 360 cm²/mg; 77°K; $\alpha = 0.55$. ↑, Adsorption of 2×10^{14} molecules/cm².

about 10%. At 77°K, after adsorption of 5×10^{14} hydrogen molecules/cm², still more gas is adsorbed, but the conductance does not show a definite change. The 273°K measurements were done on films with different surface areas. At this temperature three regions can be discerned: linear decrease in conductance with the amount adsorbed, a part in which the effect per atom adsorbed becomes continuously less, and an almost horizontal part. The slope of the initial straight part of the film with a low surface area is the same as that of the other films, but the curve declines earlier and the total decrease in conductance is only about 50% of that of the films with a large surface area. In all cases, after adsorption of about 2.2×10^{14} molecules/cm², the linear part changes into a curved part, which ends after adsorption of about 3.7×10^{14} molecules/cm².

At 373°K, the straight part goes over into the horizontal part almost immediately, and there is a definite increase in conductance on further adsorption. The linear part ends after adsorption of 2.1×10^{14} molecules/cm². A comparison of the maximum decreases in conductance of films 17, 18, 19, and 20, which have an approximately equal specific surface area, shows that the maximum decrease is the same at 77° and 273°K, but definitely lower at 373°K.

The values of the slopes of the straight parts of the experimental curves, the α values are collected in Table 4. As can be concluded from the α values obtained from measurements on films Nos. 27, 29, 30 and 26, 28 and 1.09, by the compensation method, the results are quite reproducible.

In Fig. 10 the measured isotherms for nitrogen, carbon monoxide, and hydrogen are collected. The ratio between the amounts of hydrogen adsorbed at 77° and 273°K is of the same order as that measured by Trapnell (*31*), Hickmott (*32*), and Anderson and Baker (*23*). At 273°K, the number of carbon monoxide molecules adsorbed is of the same order as the number of hydrogen molecules adsorbed.

f. The BET Surface Area of the Films

To investigate the influence of chemisorption on the BET surface area of the films, in part of the experiments the surface area is determined both before and

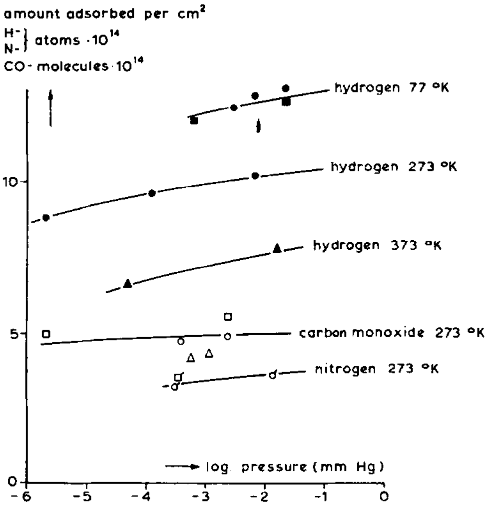

FIG. 10. Adsorption isotherms for hydrogen, carbon monoxide, and nitrogen on tungsten.

after the chemisorption. The values for the surface area of the clean films are between 330 and 495 cm²/mg of tungsten. The *c* values of the BET equation are all between 100 and 500, consequently much lower than those recorded by Anderson and Baker (*23*) at relative pressures lower than 0.04. The xenon physisorbed in the determination of the surface area has a very small (about 10^{-2} %) and irreproducible effect on the electrical resistance of the clean film. After measurement the film is heated to room temperature and the xenon can easily be pumped off.

The results of the measurements are summarized in Table 5. In a carbon monoxide experiment the surface area is determined during the chemisorption. Figure 11 shows the decrease in conductivity and in surface area. No variation in surface area is observed in the initial flat part of the conductivity curve. The decreases in surface area in oxygen and carbon monoxide adsorption are about the same, viz. 15–27%, whereas for nitrogen and hydrogen much lower values are recorded. The small decrease for nitrogen may be attributed to the fact that only a small amount is adsorbed at 273°K, viz. about 2/5 of the amount of the other gases adsorbed at this temperature.

The relatively small decrease brought about by the adsorption of hydrogen at a coverage which is about the same as that of oxygen and carbon monoxide points to the presence of narrow pores in the film. By adsorption of oxygen and carbon monoxide the pores are blocked to xenon atoms, whereas the elimination of porosity by the small hydrogen atoms is much less effective.

If the metal particles in the film should be sintered by slow dissipation of the heat of adsorption—which is improbable in view of the thermostability of the tungsten films—this would lead to a decrease for

TABLE 5
DECREASE IN BET SURFACE AREA UPON CHEMISORPTION

Film no.	Gas ads.	Adsorption temp. (°K)	Surface area before adsorption (cm² mg⁻¹)	Surface area after adsorption (cm² mg⁻¹)	Decrease (%)
1.02	O_2	77	335	275	18
1.07	O_2	77	420	305	27½
1.03	O_2	273	370	310	16
13	CO	77	380	305	15½
15	CO	77	365	275	25
16	CO	195	425	310	27
11	CO	273	495	410	17
12	CO	273	470	395	16
14	CO	273	330	250	24
22	N_2	273	375	350	6½
31	N_2	273	335	320	4½
17	H_2	77	370	345	6½
20	H_2	373	365	350	4

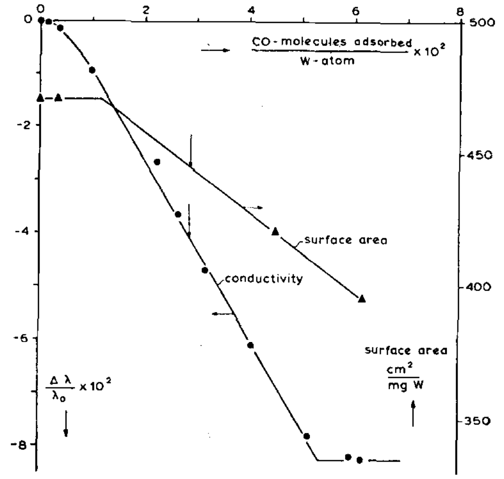

FIG. 11. Decrease in BET surface area during the adsorption of carbon monoxide. Film no. 12. ↑, Adsorption of 2×10^{14} molecules/cm².

oxygen which is markedly greater than that for carbon monoxide, owing to the higher heat of adsorption of oxygen.

III. DISCUSSION

a. Possible Mechanisms for the Influence of Adsorption on the Conductance of Evaporated Films with a Large Surface Area

As mentioned in the introduction, the change in conductance of evaporated films upon adsorption is mostly ascribed to a change in specific resistivity, while Sachtler and Dorgelo (*8*) recently pointed to the metal atoms in the surface layer losing metallic properties. In addition, other explanations have been given: changes in surface stress (*16*), and influence on electrons tunneling across gaps between the particles of the film (*33*, *16*).

It is not necessary to consider an increase in temperature brought about by slow dissipation of the heat of adsorption, as thermal equilibrium is reached each time gas is admitted. Although a change in surface stress upon adsorption may be important to some properties of evaporated metal films, the effect on the resistance appears to be too large in this case to be attributed to changes in surface stress, as has already been argued by Ehrlich (*16*). Moreover, the occurrence of a negative–positive effect on the conductance in the case of hydrogen adsorption—which is most clearly observed on evaporated nickel and iron films (*4*, *5*, *6*)—is incompatible with this explanation.

More attention should be given to the last mechanism in which a change in work function of the metal particles of the film brought about by adsorption has an influence on the tunneling of electrons across the gaps between the particles. This mechanism was first suggested by Broeder, van Reyen, Sachtler, and Schuit (*33*) and recently reviewed by Ehrlich (*16*). For our films this explanation cannot be accepted for the following reasons:

i. If the main resistance is caused by the tunneling process between isolated particles, an increase in temperature should be found to have a positive effect on the conductance (*34*). On our films a negative temperature coefficient of the conductance was always observed, if the effect of the contacts was correctly eliminated. The small value of the experimental temperature coefficients can be easily accounted for by the high residual resistivity of the films.

ii. As was measured by Mignolet (*35*), physical adsorption of xenon largely decreases the work function of tungsten. Although this influence is of the same order as that brought about by the adsorption of hydrogen, carbon monoxide, and oxygen (Table 6), no effect on the resistance is observed when xenon is adsorbed.

TABLE 6
EFFECT OF GAS ADSORPTION ON WORK FUNCTION OF TUNGSTEN

Gas	Effect on work function	Reference
O_2	+1.90	(*35*)
CO	+0.80	(*35*)
H_2	+0.48	(*35*)
Xe	−1.1	(*35*)
N_2	−0.2 to −0.1	(*36*, *37*)

iii. On copper films which are comparable with our tungsten films, Suhrmann, Ober, and Wedler (*13*) observed effects on the resistance opposite to those on the work function when carbon monoxide was adsorbed. Moreover, there is an increasing amount of evidence that nitrogen decreases the work function of tungsten upon adsorption (*36*, *37*). Therefore, nitrogen would be expected to have an effect on the conductance which is contrary to the effects of oxygen, hydrogen, and carbon monoxide, which is not the case.

iv. If, for a reasonable gap (about 10 Å), the effect of a change in work function on the tunnel resistance should be considered with reference to the theoretical prediction by Holm and Kirchstein (*38*) much greater effects on the resistance would have to be expected than those actually observed.

In summary, only a change in either the specific resistivity or the geometry of the conductive material can satisfactorily explain the experimental observations. For a proper understanding of the way in which the metal is engaged in the chemisorption process it is essential to make a decision between these two possibilities. Before a more detailed consideration will be given, we may distinguish the following two simplified viewpoints.

If the adsorbed atoms form a normal chemical bond with a distinct number of metal surface atoms, so that the atoms are converted into a condition characteristic of the chemical compound formed between the metal atom and the adsorbate, part of the metal should be changed into a state that is nonconductive or less-conductive (hydrides). This process results in a change of the geometry of the electrical conductor.

On the other hand, if after the chemisorption, the metal surface atoms should remain part of the metal and continue to contribute to the metallic properties, chemisorption changes only the specific resistivity. The adsorption bond is now formed by metal electrons in orbitals which can be described by collective wave functions of the whole metal.

In the latter case chemisorption may change the resistivity in two ways:

i. The conductivity is proportional to the concentration of the conduction electrons, and this concentration may be changed either by the metal accepting or donating electrons in the case of an ionic chemisorption bond, or by the immobilization of conduction electrons in the case of a covalent bond.

ii. When the dimensions of the metal particles in the film are of the order of the mean free path of the conduction electrons, the resistivity is increased by scattering of conduction electrons at the boundaries of the metal particles. This increase is proportional to the fraction of incident electrons which are diffusely reflected, since specular reflection has no effect on the mean free path. If this fraction of diffusely reflected electrons is altered by the chemisorption, the resistivity will also change, and this effect may outweigh the change in the number of conduction electrons.

In a recent paper by Toya (*39*) this last mechanism is given to explain the effects of hydrogen adsorption on the conductance of evaporated nickel films. Although, theoretically, very little is known at present about the reflection of conduction electrons by these boundaries, experimental evidence is against this explanation.

Reynolds and Stilwell (*40*), who measured the dependence of the resistivity on the film thickness of evaporated copper and silver films, obtained results which can only be reconciled with theoretical expectations if complete diffuse reflection is assumed. The same conclusion was drawn by Nossek (*25*, *26*) from careful experiments on evaporated alkali metal films, and by Worden and Danielson (*41*) from experiments on potassium films. Measurements of the anomalous skin effect on copper, silver, gold, tin, mercury, and aluminum (*42*, *43*) also point to complete diffuse reflection. Moreover, in our case, a change in the fraction of diffused electrons would reflect itself only in the residual resistivity. The data of Tables 2 and 3 indicate no change in the residual resistivity which is not within the experimental accuracy. We, therefore, reject this mechanism to explain our results.

b. Explanation of the Experimental Results

The most striking experimental result is that the slope of the curve showing the relative conductance versus the molecules adsorbed per metal atom is of the order of unity. Evaporated films of other metals show the same behavior (*2, 3, 6, 7*). This phenomenon can be understood from the hypothesis of either a change in resistivity (I) or a change in geometry (II), provided certain simplifying assumptions are made.

To simplify the considerations in a first approximation we assume that the effect of chemisorption of a gas molecule does not depend on the place on the film surface where it is actually adsorbed, i.e. the distribution of the admitted gas molecules over the film surface is immaterial. For a uniform concentration of conduction electrons the conductance of the clean film, λ_0, is given by

$$\lambda_0 = fn_e = f\gamma n_w$$

in which f is a proportionality constant, n_e the number of conduction electrons per unit volume, n_w the number of tungsten atoms per unit volume, and γ the average number of conduction electrons per tungsten atom. When the chemisorption of one gas molecule immobilizes X conduction electrons, and N_g gas molecules per unit volume are adsorbed, the decrease in conductance is given by:

$$-\frac{\Delta\lambda}{\lambda_0} = \frac{X}{\gamma}\frac{N_g}{n_w} = \alpha\frac{N_g}{n_w}$$

Since both X and γ are of the order of unity, the quotient $\alpha = X/\gamma$, expressing the slope of the experimental curves, is likewise of the order of unity (Mechanism I).

In the second mechanism (II) the change in conductance is due to the surface atoms losing their metallic properties by the chemisorption. The dimensions of the conductor change proportionally to the number of adatoms present at the surface of the conductor. For the slope to reach the experimental value of the order of unity and to exclude effects of the distribution of gas atoms over the film surface, it is necessary to assume a model for the porous film which consists of identical parallel cylinders, the radii of which amount to about 30 Å, as calculated from the total surface area, e.g. 350 cm²/mg.

For this model it follows by simple calculation that the slope of the curve showing $\Delta\lambda/\lambda_0$ against N_g/n_w is equal to the number of surface atoms occupied by one chemisorbed molecule, this ratio normally ranging between 1 and 2 (independent of the radius of the cylinders). If we assume that the whole surface layer should be eliminated from the conduction process the decrease in radius of the conducting cylinders, Δr, is about 1½ Å, and after full coverage:

$$-\Delta\lambda/\lambda_0 = 2\Delta r/r_0 = 0.1$$

This decrease in conductance is of the order of that actually observed.

Hydrogen adsorption would convert the surface layer into a hydride compound. From cases in which hydrogen dissolves into a transition metal—palladium is the best known example—it is known that the metallic conductivity decreases only and does not change its character after saturation with hydrogen. Hence, the decrease in the conductance and the α value are lower for hydrogen adsorption.

c. Refinement of the Designed Picture

In the foregoing considerations it was arbitrarily assumed for the sake of simplification that the distribution of the adsorbed molecules over the internal surface of the film should not affect the experimental result. A closer examination of the experimental curves, however, reveals two facts that cannot be reconciled with these assumptions, viz. the small decrease in conductance by the amounts of gas admitted first, and the increase (CO, H_2) or decrease (O_2) of the experimental α values with increasing temperature.

Obviously, the latter fact could point to a difference in bonding character of the adsorbed particles at different temperatures. However, since it is known from field-emission and flash-filament experiments (*44, 32, 45, 46, 36*) that the transition between differently bonded species is extremely rapid, a thermodynamic equilibrium between the different particles would be expected. But we find that the addition of CO at high temperature gives a high value of α even when measured at low temperature. Suhrmann, Mata Arjona, and Wedler (*15*) furthermore find an increase of α after addition of CO at low temperature, heating to 273°K, and recooling. For oxygen we find that addition at low temperature also determines the α value at the higher temperature.

Moreover, in flash-filament experiments (*32, 45, 46, 47*), the presence of differently bound species is recorded only at coverages at which more than 25% of the total adsorbable amount is taken up. In our experiments the difference in α values is already present at coverages that are much lower, if the coverages are calculated on the assumption that the admitted gas molecules are homogeneously distributed over the total metal surface. We therefore believe that other explanations must be sought, since, as said above, kinetic effects are also excluded.

As was proved by accurate blank measurements, the relatively small effects on the conductance of the amounts of gas admitted first is not due to adsorption of gas in the cold trap or on the baked glass of the measuring cell. Moreover, as can be concluded from the data of Table 7, the amount of CO adsorbed in this stage is roughly proportional to the total film weight, and, therefore, this adsorption must reflect an intrinsic property of the experimental films.

TABLE 7

Amount of Carbon Monoxide Adsorbed with Small Effect on the Conductance

Film no.	Film weight (mg)	Surface area (cm² mg⁻¹)	Total amount of gas adsorbed in this stage (molecules × 10¹⁷)	Amount of gas adsorbed per cm² of tungsten (molecules × 10¹⁴/cm²)
9	18.3	270	7.32	1.48
13	9.4	305	4.06	1.41
15	3.9	275	1.36	1.27

We believe that both the variation of α with temperature and the occurrence of an "initial flat section" which is proportional to the weight of the film point to an inhomogeneous covering of the interior film surface with adsorbed gas atoms, and show that the effect of adsorption on the conductance is not completely independent of the place on the surface where the adatoms stick.

We consequently have to develop a less simplified film structure which can account for these facts and moreover explain the experimental values for the geometric factor, which values were found to increase with film thickness from 2 to 3.

These requirements are not fulfilled by the simple model of a porous film structure consisting of more or less uniform particles connected by small necks, as suggested by Ehrlich (*16*).

In this case, only adsorption on the neck surfaces would affect the conductance of the film. Since, however, both the change-in-resistivity and the change-in-geometry model point to conductance-determining metal particles with a surface-to-volume ratio of the same order of magnitude as the average surface-to-volume ratio of the total film, this model should require very long necks connecting rather large metal particles, which is a very unrealistic situation.

Furthermore, this model cannot explain the fact that the conductance-determining parts of the film are generally situated in places difficult of access from the gas phase.

We believe that the following model eliminates these difficulties: The experimental films are composed of porous clusters of small metal particles intimately grown together. These clusters are connected by isolated metal particles of the same dimensions as the particles present in the clusters. Only chemisorption on the surfaces of these bridging particles has a marked effect on the conductance of the film.

In order to account for the ratio of the experimental and the ideal geometric factors of the films, we will set up the following schematical model.

The porous clusters of small metal particles have a uniform size of dimension D, and 50% porosity. The over-all resistance of the film is determined by the dimension d of an average number of n particles between each two clusters.

It can easily be shown that the resistance of a film with a length l and a width b equals:

$$R = (l/bnd) \cdot \rho_{\text{spec}}$$

while the resistance of a compact film of the same weight on the same substrate is equal to:

$$R = (2l/bD) \cdot \rho_{\text{spec}}$$

From these expressions it follows that the ratio of experimental and ideal geometric factors can be given by:

$$G_{\text{exp}}/G_{\text{id}} = D/2nd$$

A comparison with the experimental value of 2–3 reveals that, for $D/d = 10$, n is ~ 2, values which do not seem unacceptable.

FIG. 12. Model of the experimental films.

The particular model chosen readily accounts for the fact that the experimental α values are close to unity. The surface/volume ratio of the conductance-determining elements is equal to that of the whole film. Furthermore, the effects of the inhomogeneous distribution of the adatoms over the inner surface of the film can be easily understood from this model. The amounts of gas admitted first will be largely retained on the outer part of the chemisorbing metal film where they have hardly any influence on the conductance because of the low mobility over the surface at low coverages and temperatures and the relatively high values of the sticking probability (the probability that an incident gas molecule is chemisorbed) under these conditions. The gas molecules cannot reach the conductance-determining elements until the sticking probability has decreased considerably.

Hence, the range over which the effect of chemisorption on the conductance is only small must be reflected in the sticking probabilities of the several gases studied. Although the values obtained for these sticking probabilities by various authors do not agree very well, the gases may be classified in this order (Table 8):

$$CO > O_2 > N_2 > H_2$$

TABLE 8
STICKING PROBABILITIES ON CLEAN TUNGSTEN SURFACES

Gas	Sticking probability	References
CO	0.3–0.6	(*46–69*)
O_2	0.2–0.5	(*49–51*)
N_2	0.1–0.4	(*45, 48, 49*)
H_2	0.1	(*32*)

The same order is observed for the size of the initial flat section.

The measurement of oxygen adsorption at 77°K indicates physical adsorption on top of the chemisorbed layer without further oxidation, since after a coverage of 4×10^{14} molecules/cm^2 the adsorption is no longer accompanied by a further decrease in conductance (Fig. 4). This is confirmed by the experiment of Fig. 5: At the end of the steep linear decrease in conductance, admission and adsorption of oxygen at 77°K do not affect the conductance, whereas during heating to 273°K oxygen is temporarily desorbed and again slowly taken up with a further decrease in conductance, which remains after cooling to 77°K.

The slow uptake of oxygen at 273°K, which brings about a smaller decrease in conductance per oxygen molecule, apparently corresponds to the further oxidation of the surface already covered with a monolayer.

The lower α values found in the experiment in which oxygen is admitted at 273°K must be ascribed to the combination of chemisorption and further oxidation of readily accessible parts of the film, while the less accessible parts still remain uncovered. Accordingly, higher α values are recorded at 77°K and 196°K, when no further oxidation occurs, than at 273°K, whereas after distribution of the admitted oxygen over the surface at 77°K the same high α values are measured at 273°K as at lower temperatures. This oxidation during the transport of oxygen to the uncovered parts of the surface also explains the fact that at the end of the steep linear decrease more oxygen is taken up at 273°K than at 77°K and 196°K.

In the case of CO adsorption the effect of temperature on the α value is caused by the mobility of the chemisorbed species over the surface towards the conductance-determining elements. As shown by Klein (*52*) and Ehrlich (*36*), this mobility sets in at temperatures of about 200°K when the coverage is sufficiently high for the "α state" to be reached. At lower coverages, when only the "β state" exists, mobility is zero below 625°K.

This explanation is confirmed by the observation that, although upon addition of a new amount of CO adsorption takes place almost immediately, the conductivity decreases slowly, which shows that the adsorbed molecules migrate to the less accessible conductance-determining elements of the film. Also the results obtained by Suhrman and Wedler (*53*) demonstrated this slow migration of adsorbed CO molecules on *nickel* films.

The temperature influence is enlarged by the fact that the surfaces of narrow pores can be reached only by gas molecules that have migrated over the surface. As is evident from the decrease in BET surface area after chemisorption, the experimental films possess pores the entrance to which is blocked to xenon atoms by adsorbed molecules, and also to new impinging CO molecules, unless a certain degree of mobility is reached.

Therefore, part of the conductance-determining particles are not covered at 77°K and, to a less extent, at 195°K, so that both the total decrease in conductance and the α values observed are lower. These narrow pores, which are apparently present in evaporated metal films, also bring about the maximum in the irreversible ascending branch of the adsorption isobar which was observed for hydrogen and carbon monoxide by various authors (*54, 55, 31*). These authors ascribed this phenomenon to slow absorption into the metal for hydrogen and to carbonyl formation for carbon monoxide. Gundry and Tompkins (*56*) proved it to be a surface effect at low temperatures. They attributed it to the presence of a more weakly bound precursor chemisorbed state from which the molecules entered into the final adsorbed state with an activation energy increasing with increasing coverage.

All these explanations are ruled out by the flash-filament experiments on hydrogen chemisorption carried out by Hickmott (*32*). At all temperatures studied he observed an equilibrium, which was rapidly attained on his filament samples which had no narrow pores. For carbon monoxide this behavior was observed by Ehrlich (*46*). The explanation offered here, e.g. the presence of narrow pores blocked at the entrance as long as the mobility is insufficient, has also been suggested by Ponec and Knor (*57*) for hydrogen on nickel films.

The results of hydrogen adsorption can be explained along the same lines, but, owing to the lower adsorption energy, the equilibrium coverage also changes with temperature.

As is reported by Gomer, Wortman, and Lundy (*44*), the activation energy for the migration of adsorbed hydrogen over tungsten increases with decreasing coverage. At the highest coverages mobility in the chemisorbed layer is observed above 180°K, whereas at lower coverages higher temperatures are required to mobilize the adsorbed hydrogen atoms. This implies that at 77°K the distribution of the hydrogen is very inhomogeneous, which results in a low α value.

Trapnell (*31*), on evaporated tungsten films, and Hickmott (*32*), on tungsten filaments, observed that the amount of chemisorbed hydrogen depends on the temperature; our measurements represented in Fig. 10 show the same pattern. As more hydrogen is chemisorbed, the conductance of the film will become lower. Consequently, the total decrease in conductance is lower at 373°K than at 273°K. At 77°K, the inaccessibility of the narrow pores balances the effect of the larger chemisorption, and, hence, the total decrease in conductance is about the same as at 273°K.

As known from flash-filament experiments (*45*) at room temperature, nitrogen is adsorbed on tungsten mainly in the "β state." From an analysis of the desorption characteristics (*58*) Ehrlich concluded that in this state the nitrogen is atomically bound (*59*). At temperatures of about 100°K a much more weakly bound "γ state" is present besides this strongly adsorbed entity. When the adsorption is completely carried out at 115°K, the ratio n_β/n_γ is 0.41, whereas, after presaturation of the surface at 300°K, n_β/n_γ is about unity (*45*). Finally, it appeared from field emission that below 400°K the adsorbed nitrogen does not move over the surface (*36*). An inhomogeneous distribution is therefore to be expected on our film.

From Fig. 8 it can be concluded that after saturation at 273°K an approximately equal amount of nitrogen can still be adsorbed at 77°K with only a slight decrease in conductance. If this additional amount of nitrogen is associated with "γ-adsorbed" nitrogen, it follows that nitrogen adsorbed in this way has hardly any effect on the conductance, whereas the "β-adsorbed" nitrogen has a strong effect. When nitrogen is admitted to a tungsten film at 77°K, a large part of the gas will be adsorbed in the "γ-state" and, consequently, a very low α value will be observed, the total decrease in conductance also being low. When, after saturation at 77°K, the film is heated to room temperature, the "γ-state" adsorbed nitrogen is partly desorbed and partly adsorbed in the "β state," which results in a further decrease of the conductance. Upon recooling, the total amount of nitrogen is again taken up, but now the n_β/n_γ ratio has increased and the conductance has further decreased accordingly.

d. Conclusions about the Bonding of the Gas Atoms to the Metal Surface

The foregoing discussion has indicated that it will be difficult to draw quantitative conclusions about the bonding character of different adsorbed molecules from experimentally derived α values. Only under those conditions where the effects of an inhomogeneous distribution are virtually absent do the experimental data give information about the actual situation on the conductance-defining elements. It has been shown that under these conditions the order of magnitude of these α values differs from gas to gas and amounts to:

H_2	α = ca. 1.0
CO	α = ca. 2.2
O_2	α = ca. 2.6
N_2	α = ca. 3.9

A first glance at these figures shows a striking correlation with the chemical valency of the adatoms involved: The $\alpha_{N_2}/\alpha_{O_2}$ ratio 1.5 and also the value of α_{H_2} are not very far from the expected value for a monovalent adatom. Serious difficulties arise, however, in explaining the value found for CO on this basis, as no indications of a bonding type, except the carbonyl bond, are known, so that the α_{CO} seems to be too high. This seems to necessitate a closer analysis of the experimental data in the light of the theories of metallic conductivity.

Although the theory of the metallic conductivity, especially of transition metals, is only poorly developed quantitatively, the physical principles underlying the conduction phenomenon are well understood at present (*60*). A requisite for metallic conductivity in a solid is the presence of a periodic potential. In addition, part of the electrons must be present in orbitals collective of the whole solid with a quasi-continuous range of energy levels, i.e. energy bands which are not completely filled.

In such a periodic structure the interactions between the electrons are relatively unimportant and, except at extremely low temperatures, the resistance is due to thermal vibrations of the metal atoms (*61*). The scattering of the conduction electrons by the atom cores is proportional to $\bar{R}^2$, the mean square of the deviation from the equilibrium position. $\bar{R}^2$ is proportional to the temperature, and, consequently, if no other variables are changed (viz., the number of conduction electrons or the cohesive properties of the solid) the resistance is proportional to the temperature.

For transition metals the collective electrons are present in two overlapping energy bands, one derived from atomic *d* orbitals and one from atomic *s* orbitals. In the *d* band the electrons are about a factor 10 less mobile than in the *s* band (*60*). Since the density of states in the *d* band is much higher than that in the *s* band, a large contribution to the electrical resistance results from scattering of *s* electrons into the *d* band. This explains the relatively low conductivity of the transition metals.

The phenomena occurring when an atom with a different valency is placed inside a metal are extensively investigated by Friedel (*62, 63*). The potential of the foreign ion core, which deviates from the potentials of the other metal atoms, is shielded over a short distance by the collective electrons of the metal (*61*). Especially in transition metals this shielding is very effective owing to the high density of states of the *d* band and the potential difference is leveled out to about one Ångström. [Ziman, however, states that, owing to the high effective mass of *d* electrons, their contribution to the shielding remains small (*64*)].

This implies that also after chemisorption the influence on the metal properties is restricted to the direct environment of the chemisorbed atom. Consequently, the band structure within the metal will not change on adsorption.

Although the structure of the metal surface will differ from the bulk structure due to the presence of unsaturated bonds, it retains a two-dimensional periodicity and, hence, a metallic conductivity. In the above the decrease in conductance upon adsorption was ascribed to either a transfer into a nonconductive state of the surface layer or a change in specific conductivity. As has already been discussed, the last mechanism must be replaced by a change in specific conductivity of the surface layer only. When the interaction between an adsorbed atom and the metal surface is considered in more detail, the following may be found to occur upon chemisorption:

i. The average number of *s* electrons in the surface layer changes; this change in the number of current carriers leads to a change in surface conductivity.

ii. The average number of *d* electrons in the surface layer changes; then the scattering properties of the *d* states are altered.

iii. The bonds that bind the surface atoms to the remaining part of the metal are changed; then, the amplitude of the thermal vibrations is altered and, consequently, also the scattering of the conduction electrons.

iv. The structure of the surface is so severely distorted that electrical conductance is no longer possible by loss of the periodicity. Inasmuch as the displacements that bring about the scattering in the thermal vibrations are rather small [for tungsten at 300°K $\bar{R}^2 = \sim 10^{-19}$ cm^2 (*65*)], it may be concluded that displacements of about 0.1 Å are enough to destroy the conductivity completely.

Obviously, definite conclusions can only be reached if one and the same mechanism operates for all different gases studied. There are indications, however, that this is not true. That at least *i.* and *ii.* must be operative together is most clearly demonstrated by the influence of chemisorption on the metallic properties of nickel. Measurements on small nickel particles indicated unambiguously that chemisorption of hydrogen, carbon monoxide, and oxygen (*66, 67, 68*) decreases the magnetization of the nickel particles, and, consequently, affects the *d* electrons of the metal. On the other hand, carbon monoxide (*6, 7*) and oxygen (*7, 12*) adsorption decrease the conductance of evaporated nickel films, in a way analogous to that observed for tungsten, while hydrogen adsorption first decreases the conductance (*4, 5, 6, 11*) and then somewhat restores it. As *d* electrons contribute negligibly to the conductivity, this implies that both *s* and *d* electrons of the metal must be affected by chemisorption.

Furthermore, it is felt that the influence on the remaining intermetallic bonds of the surface atoms is largely dependent on the adsorption energy of the particular chemisorbed species involved.

When hydrogen is bonded to a tungsten surface, resonating bonds with three or more surface atoms are established (*69, 70, 71*). It is assumed that this bonding is not strong enough to lift the surface atoms appreciably from their equilibrium positions; the intermetallic bonding is somewhat weakened and, consequently, the amplitude of the vibrations of the metal atoms is increased. As a result, the conductance is decreased by the adsorption to a relatively small extent. Probably, also the *s* and *d* electrons are influenced to some extent, but any statement about this effect will be highly conjectural for the time being. The change in slope of the conductivity vs. coverage curves at 273°K may be related to Becker's (*69*) observations that at low coverages specifically weakly bound tungsten atoms are covered, whereas at higher coverages more strongly bound surface atoms are involved.

On the other hand, bonding of oxygen, carbon monoxide, and nitrogen will have a stronger influence on the intermetallic forces and displace the surface atoms further from their equilibrium positions. This can reasonably be explained from the higher adsorption energies and activation energies needed by these gases to migrate in the chemisorbed state. We therefore accept that on adsorption of oxygen, carbon monoxide, and nitrogen the metal atoms to which the gas atoms are bound will lose their conductive properties. The experimental data indicate that at full coverage one oxygen molecule and one CO molecule each displace two tungsten surface atoms. This explains why the α_{CO} and α_{O_2} are of the same order of magnitude. The somewhat smaller value for carbon monoxide may be ascribed to the presence of the more weakly bound "α state," which has no strong effect on the intermetallic distance. Redhead (*47*) raised strong arguments for the "α-bonded" molecules filling gaps in the surface covered with "β-bonded" carbon monoxide. Since about 10% of these gaps may be expected in the "β-covered" surface, the difference in α values is quite reasonable.

It is shown by field ion-emission experiments that at 273°K nitrogen is only adsorbed on atomically rough surfaces, whereas the densely packed {110} planes remain uncovered (*78*). This is also apparent from the results recently obtained from surface potential measurements on tungsten covered with nitrogen (*36, 37*). If appropriate precautions are taken against contamination from carbon monoxide, nitrogen adsorption appears to decrease the work function of tungsten. As the electronegativity of nitrogen is of the same order of magnitude as that of hydrogen and oxygen, which increase the work function, this can only be explained if it is assumed that nitrogen is adsorbed below the level of the outer tungsten surface atoms (*72*). This is only possible on atomically rough surfaces. The ratio $\alpha_{N_2}/\alpha_{CO} = 3/2$ suggests the elimination from the conduction process of three tungsten surface atoms per adsorbed nitrogen atom. Since nitrogen is only adsorbed on sites where it may come into contact with more than two metal surface atoms, this accordance with chemical valency is reasonable.

Owing to the presence of {110} planes, where nitrogen is not adsorbed at 273°K, the saturation coverage of this gas is smaller than 2/3 of the amount of oxygen adsorbed in a monolayer. As was to be expected, the weakly adsorbed "γ nitrogen" does not influence the metal structure and, hence, no effect on the conductance is observed.

Besides accounting for the effects on the conductance, the assumption that the metal atoms are displaced to a greater or smaller extent from their equilibrium lattice sites upon chemisorption also gives an easy explanation of the effects of adsorption on ferromagnetic properties (*66*, *67*, *68*). Probably, ferromagnetism is more susceptible to the distance between the metal atoms than the electrical conductivity. When this distance is sufficiently altered by chemisorption, the metal atoms engaged in the chemisorption stop to contribute to the collective ferromagnetism of the metal.

ACKNOWLEDGMENT

The authors are much indebted to Mr. van Cleef who very skillfully constructed and reconstructed the apparatus in which these measurements were carried out.

REFERENCES

1. Sachtler, W. M. H., *J. Chem. Phys.* **25**, 751 (1956).

2. van Heerden, C., and Zwietering, P., *Koninkl. Ned. Akad. Wetenschap. Proc. Ser. B.* **60**, 160 (1957).

3. Suhrmann, R., Wedler, G., and Genetsch, H., *Z. Physik. Chem.* (*Frankfurt*) **17**, 350 (1958).

4. Sachtler, W. M. H., and Dorgelo, G. J. H., *Bull. soc. chim. Belges* **67**, 465 (1958).

5. Suhrmann, R., Mizushima, Y., Hermann, A., and Wedler, G., *Z. Physik. Chem.* (*Frankfurt*) **20**, 332 (1959).

6. Zwietering, P., Koks, H. L. T., and van Heerden, C., *J. Phys. Chem. Solids* **11**, 18 (1959).

7. Suhrmann, R., Wedler, G., and Heyne, H. J., *Z. Physik. Chem.* (*Frankfurt*) **22**, 336 (1959).

8. Sachtler, W. M. H., and Dorgelo, G. J. H., *Z. Physik. Chem.* (*Frankfurt*) **25**, 69 (1960).

9. Mizushima, Y., *J. Phys. Soc. Japan* **15**, 1614 (1960).

10. Gr'aznov, V. M., Chimulis, V. I., and Yagodovskii, V. D., *Dokl. Akad. Nauk SSSR* **132**, 1132 (1960).

11. Ponec, V., and Knor, Z., *Collection Czech. Chem. Commun.* **25**, 2913 (1960).

12. Wedler, G., *Z. Physik. Chem.* (*Frankfurt*) **27**, 388 (1961).

13. Suhrmann, R., Ober, H., and Wedler, G., *Z. Physik. Chem.* (*Frankfurt*) **29**, 305 (1961).

14. Suhrmann, R., Krüger, G., and Wedler, G., *Z. Physik. Chem.* (*Frankfurt*) **30**, 1 (1961).

15. Suhrmann, R., Mata Arjona, A., and Wedler, G., *Z. Elektrochem.* **65**, 786 (1961).

16. Ehrlich, G., *J. Chem. Phys.* **35**, 2165 (1961).

17. Bennett, M. J., and Tompkins, F. C., *Trans. Faraday Soc.* **53**, 185 (1957).

18. Podgurski, H. H., and Davis, F. N., *J. Phys. Chem.* **65**, 1343 (1961).

19. Venema, A., and Bandringa, M., *Philips Tech. Rev.* **20**, 97 (1958).

20. Mayer, H., "Physik Dünner Schichten," p. 221. Wissenschaftliche Verlagsgesellschaft, mbH Stuttgart, Germany, 1955.

21. Brunauer, S., Emmett, P. H., and Teller, E., *J. Am. Chem. Soc.* **60**, 309 (1938).

22. Livingston, H. K., *J. Colloid Sci.* **4**, 447 (1949).

23. Anderson, J. R., and Baker, B. G., *J. Phys. Chem.* **66**, 482 (1962).

24. Mott, N. F., and Jones, H., "The Theory of the Properties of Metals and Alloys," p. 286. Dover, New York, 1958.

25. Mayer, H., in "Structure and Properties of Thin Films" (C. A. Neugebauer, J. B. Newkirk, and D. A. Vermilyea, eds.), p. 225, p. 254. Wiley, New York, 1959.

26. Nossek, R., *Z. Naturforsch.* **16a**, 1162 (1961).

27. Gerritsen, A. N., *in* "Encyclopedia of Physics" (S. Flügge, ed.), Vol. 19, p. 156. Springer Verlag, Berlin, 1956.

28. Mayer, H., "Physik Dünner Schichten," p. 266. Wissenschaftliche Verlagsgesellschaft mbH Stuttgart, 1955.

29. Cottrell, A. H., "Theoretical Structural Metallurgy," p. 184. Edward Arnold (Publishers) Ltd., London, 1955.

30. Pierotti, R. A., and Halsey, G. D., *J. Phys. Chem.* **63**, 680 (1959).

31. Trapnell, B. M. W., *Proc. Roy. Soc.* (*London*) *Ser.* **A206**, 39 (1951).

32. Hickmott, T. W., *J. Chem. Phys.* **32**, 810 (1960).

33. Broeder, J. J., van Reijen, L. L., Sachtler, W. M. H., and Schuit, G. C. A., *Z. Elektrochem.* **60**, 841 (1956).

34. Neugebauer, C. A., and Webb, M. B., *in* "Electric and Magnetic Properties of Thin Metallic Layers" (L. van Gerven, ed.) p. 37. Koninklijke Vlaamse Akademie van Wetenschappen, Letteren en Schone Kunsten van België, Brussel, Belgium, 1961.

35. Mignolet, J. C. P., *Rec. trav. chim.* **74,** 685 (1955).
36. Ehrlich, G., and Hudda, F. G., *J. Chem. Phys.* **35,** 1421 (1961).
37. Hill, M. P., and Pethica, B. A., *J. Chem. Phys.* **36,** 3095 (1962).
38. Holm, R., and Kirchstein, B., *Z. Tech. Physik.* **11,** 488 (1935).
39. Toya, T., *J. Res. Inst. Catalysis, Hokkaido Univ.* **8,** 209 (1961).
40. Reynolds, F. W., and Stilwell, G. R., *Phys. Rev.* **88,** 418 (1952).
41. Worden, D. G., and Danielson, G. C., *J. Phys. Chem. Solids* **6,** 89 (1958).
42. Sondheimer, E. H., *Adv. in Phys.* **1,** 1 (1952).
43. Smith, G. E., *in* "The Fermi-Surface" (W. A. Harrison and M. B. Webb, eds.), p. 182. Wiley, New York, 1960.
44. Gomer, R., Wortman, R., and Lundy, R., *J. Chem. Phys.* **26,** 1147 (1957).
45. Ehrlich, G., *J. Chem. Phys.* **34,** 29 (1961).
46. Ehrlich, G., *J. Chem. Phys.* **34,** 39 (1961).
47. Redhead, P. A., *Trans. Faraday Soc.* **57,** 641 (1961).
48. Ricca, F., Nasini, A. G., and Saini, G., *J. Catalysis* **1,** 458 (1962).
49. Schlier, R. E., *J. Appl. Phys.* **29,** 1162 (1958).
50. Eisinger, J., *J. Chem. Phys.* **30,** 412 (1959).
51. Becker, J. A., Becker, E. J., and Brandes, R. G., *J. Appl. Phys.* **32,** 411 (1961).
52. Klein, R., *J. Chem. Phys.* **31,** 1306 (1959).
53. Suhrmann, R., and Wedler, G., *Z. Elektrochem.* **63,** 748 (1959).
54. Beěck, O., Ritchie, A. W., and Wheeler, A., *J. Colloid Sci.* **3,** 505 (1948).
55. Rideal, E. K., and Trapnell, B. M. W., *Proc. Roy. Soc. (London) Ser.* **A205,** 409 (1951).
56. Gundry, P. M., and Tompkins, F. C., *Trans. Faraday Soc.* **53,** 218 (1957).
57. Knor, Z., and Ponec, V., *Collection Czech. Chem. Commum.* **26,** 37 (1961).
58. Becker, J. A., and Hartman, C. D., *J. Phys. Chem.* **57,** 153 (1953).
59. Ehrlich, G., *J. Phys. Chem.* **60,** 1388 (1956).
60. Jones, H., *in* "Encyclopedia of Physics" (S. Flügge, ed.) Vol. 19, p. 227. Springer Verlag, Berlin, Germany, 1956.
61. Raimes, S., *Repts. Progr. Phys.* **20,** 1 (1957).
62. Friedel, J., *Phil. Mag.* **43,** 153 (1952).
63. Friedel, J., *Adv. in Phys.* **3,** 446 (1954).
64. Ziman, J. M., "Electrons and Phonons," p. 170. Oxford at the Clarendon Press, London, 1960.
65. Jones, H., *in* "Encyclopedia of Physics" (S. Flügge, ed.) Vol. 19, p. 242. Springer Verlag, Berlin, Germany, 1956.
66. Schuit, G. C. A., and van Reijen, L. L., *Adv. in Catalysis* **10,** 271 (1958).
67. Leak, R. J., and Selwood, P. W., *J. Phys. Chem.* **64,** 1114 (1960).
68. Geus, J. W., Nobel, A. P. P., and Zwietering, P., *J. Catalysis* **1,** 8 (1962).
69. Becker, J. A., *in* "Actes du Deuxième Congrès Internationale de Catalyse," p. 1777. Éditions Technip, Paris, France, 1961.
70. Takaishi, T., *Z. Physik. Chem. (Frankfurt)* **14,** 164 (1958).
71. Pliskin, W. A., and Eischens, R. P., *Z. Physik. Chem. (Frankfurt)* **24,** 11 (1960).
72. Ehrlich, G., and Hudda, F. G., *J. Chem. Phys.* **36,** 3233 (1962).